

**A Preliminary Study Measuring the Number of T-Cell
Receptor-Rearrangement Excision Circles (TRECs) in Peripheral Blood
T-Cell Populations of A-Bomb Survivors and Control Populations**

Yoshiko Kubo M.T., Mika Yamaoka C.C., Yoichiro Kusunoki Ph.D.

Department of Radiobiology/Molecular Epidemiology
Radiation Effects Research Foundation, Hiroshima, Japan

CYTOMETRY RESEARCH

Vol.16-1 (Mar., 2006) 別刷

原著

A Preliminary Study Measuring the Number of T-Cell Receptor-Rearrangement Excision Circles (TRECs) in Peripheral Blood T-Cell Populations of A-Bomb Survivors and Control Populations

Yoshiko Kubo M.T., Mika Yamaoka C.C., Yoichiro Kusunoki Ph.D.

原爆被爆者末梢血T細胞集団および対照集団におけるT-Cell Receptor-Rearrangement Excision Circles (TRECs) の測定に関する予備的研究

久保 美子, 山岡 美佳, 楠 洋一郎

放射線影響研究所 放射線生物学/分子疫学部

原爆放射線による免疫系の障害を被った被爆者では、半世紀以上経た今日においてもナイーブCD4 およびCD8T細胞の割合の低下が認められている。今回、被爆者におけるナイーブT細胞集団の減少が胸腺でのT細胞産生の低下によるものか検討する目的で、原爆被爆者末梢血T細胞集団におけるT-cell receptor-rearrangement excision circles (TRECs) を測定するリアルタイムPCR法の確立を試みた。研究室内の対照を用いて行ったリアルタイムPCRでは、良好な再現性でTRECのDNA配列を定量的に検出することができた。これまでに測定を完了した445名について、性、年齢、および被ばく線量を変量とした多重回帰解析を行ったところ、CD4 T細胞集団におけるTREC数は女性で有意に多く、男女とも加齢につれ有意に減少した。また、被爆時の年齢が20歳未満の対象者では、被ばく線量の増加とともに低下する傾向 ($p = 0.09$) が示唆された。CD8 T細胞集団においても同様の性差および加齢の影響が認められたが、有意な放射線の影響は観察されなかった。これらの結果は、原爆放射線被ばくによる胸腺でのCD4 T細胞産生の長期低下の可能性を支持する。この仮説を検証するためには、さらに対象者数を拡大して調べる必要がある。

Keywords: TREC, immune system, radiation, aging

Abstract

More than a half century after damage of the immune systems by the radiation from A-bomb, we can still observe significant decreases in the percentages of naïve CD4 and CD8 T cells among the survivors. To investigate whether the observed decreases in the naïve T-cell

populations may have resulted from reduction in thymic T-cell production ability of survivors, we established a real-time PCR method to examine the number of T-cell receptor-rearrangement excision circles (TRECs) in peripheral blood CD4 and CD8 T-cell populations. The real-time PCR quantitatively detected TREC sequences with a good reproducibility in human laboratory controls. In the 445 survivors so far been examined, multiple regression analysis indicated that the number of TRECs in the CD4 T-cell fraction was significantly higher in

Department of Radiobiology/Molecular Epidemiology
Radiation Effects Research Foundation, Hiroshima, Japan

受付日:平成17年9月14日 受理日:平成17年10月17日

females than in males and decreased significantly with age in both males and females. This analysis also suggested a possible dose-dependent decrease in the number of TREC_s in the CD4 T-cell fraction of the survivors who were less than 20 years of age at the time of bombing ($p = 0.09$). A similar statistically significant trend for gender difference or age was observed in the CD8 T-cell fraction of the survivors. However, there was no effect of radiation exposure on the number of TREC_s in the CD8-T cell fraction. The results indicate the possibility that A-bomb radiation exposure may have induced a long-term impairment in thymic CD4 T-cell production. Further investigations in a larger study population are necessary to test this hypothesis.

Introduction

Advancing age is accompanied by a variety of alterations in the immune system that can increase the susceptibility of affected individuals to certain diseases. Particularly, age-dependent decreases of T lymphocyte count and function can lead to persistent infections and chronic inflammation. Especially, deficits of the naïve T-cell population may diminish the capability of the host immune system to defend against intrusion of pathogens to which the person has not been previously exposed¹¹. Our earlier immunological studies on A-bomb survivors have shown that percentages of naïve CD4 and CD8T cells in peripheral blood lymphocytes are significantly decreased in a radiation dose-dependent manner almost 60 years after the bombing¹⁵. This may indicate that the naïve T-cell pools poorly recovered after radiation-induced damage of the T-cell system and have never returned to the normal level. Two distinct mechanisms are involved in ensuring immune reconstitution after T-cell depletions, such as those due to radiation or chemotherapy⁹. The first mechanism depends upon renewed proliferation of the survived mature T cells that can repopulate the memory T-cell pool, whereas the second relies upon the differentiation of hematopoietic stem cells into new T cells that comprise the naïve T-cell pool. Therefore we hypothesized that an impairment of the ability to maintain normal-sized naïve-CD4 T-cell pools in A-bomb survivors could have resulted from an insufficient supply of new CD4 T cells from the thymus.

It has become possible to be enumerated the peripheral blood $\alpha\beta$ T cells that have recently emigrated from the thymus without having experienced cell divisions in the periphery by quantifying T-cell receptor-rearrangement excision circles (TREC_s) generated during T-cell receptor (TCR) gene rearrangement in the thymus¹³. TREC_s can be specifically amplified by PCR using primers that anneal to sequences adjacent to the joining signal ends of the DNA excised from the TCR $\alpha\delta$ locus and can be quantified by competitive PCR or real-time PCR^{1,2,10}. Because the excised DNA is not replicated and lost in daughter cells, TREC_s can be detected primarily in naïve T-cell populations but most merely in memory T cells¹. Recent studies using quantification of TREC_s in humans suggest that thymic function that produces T cells declines with age^{1,2}. Further, in patients infected with HIV-1, the thymic function decreases with progression of the viral burden but can recover to some extent after high active antiretroviral therapy¹. We therefore assumed that A-bomb radiation may have accelerated age-dependent thymus involution and expected to find that the numbers of T cells with TREC_s would be somewhat lower in A-bomb exposed survivors than in age-matched but non-exposed controls. In the present study we are examining the number of TREC_s in peripheral blood T-cell populations among A-bomb survivors to test the hypothesis that abnormal decreases in the naïve T-cell populations may have resulted from reduction in thymic T-cell production ability of the survivors, specifically as related to radiation.

Materials and methods

Blood donors

Blood samples were obtained from members of a survivor cohort in which 1,280 survivors had been selected, as they distributed almost equally by age, gender, and radiation dose, from Hiroshima participants in the Adult Health Study (AHS) at the Radiation Effects Research Foundation (RERF) in 1992⁸. The selected study population consists of Hiroshima survivors who were exposed to radiation doses of ≥ 0.005 Gy (0.005-4 Gy) within two kilometers of the hypocenter and a second group who were > 3 km from the hypocenter (i.e., exposed to background doses). The radiation doses are based on DS02¹². Each participant is invited to have clinical examination at

RERF every 2 years. For the present study, blood samples were obtained with the informed consent of the survivors and analyzed between May 2003 and May 2005. Besides the survivors, samples from several laboratory controls (five males aged 38-60, and two females aged 39 and 43) were also obtained with the informed consent. Mononuclear cell fractions were separated by the Ficoll-Hypaque gradient technique⁷⁾ and used for analyses.

Isolation of CD4 and CD8 T-cell populations

Approximate ten million mononuclear cells were stained with 10 μ l of FITC-labeled CD4 antibody (BD Biosciences, San Jose, CA, USA) and 25 μ l PE-Cy5-labeled CD8 (BD-PharMingen, San Diego, CA, USA) in 200 μ l of PBS containing 1% FCS for 30 min on ice. The cells were washed and resuspended in PBS containing 1% FCS and 0.1% sodium azide, and applied to a FACS Vantage SE (BD Biosciences). Each CD4 and CD8 T-cell fraction was separated and collected into a tube containing 100 μ l of PBS plus 1% BSA (Sigma-Aldrich, St. Louis, MO). In some experiments, approximate ten million mononuclear cells were stained with 10 μ l of FITC-labeled CD4 antibody and 0.5 μ l of PE-labeled CD45RA antibody (Coulter-Immunotech, Marseille, France), and CD4⁺ CD45RA⁺ naïve and CD4⁺ CD45RA⁻ memory T-cell fractions were similarly separated by the FACS Vantage SE. The collected cells were washed with PBS and centrifuged with 3,000 rpm for 5 minutes, the supernatants were removed, and the cell pellets were stored at -20 °C until used for TREC measurement.

Measurement of TREC numbers

The number of TRECs in 1 x 10⁵ cells from each fraction were enumerated by the method reported by Yasunaga, et al¹⁶⁾. The procedure was modified to use crude DNA extracts resulting from a single treatment with proteinase K, which proved to be suited to accurate quantification of the TRECs. In brief, 7 μ l (7 μ g) of proteinase K (Sigma-Aldrich) was used per 10⁵ cell pellets, and the cells were digested at 56 °C for 2 hr in the presence of 0.02% NP-40, 50mM KCl, 10mM Tris-HCl (pH 8.4) and then incubated at 95 °C for 30 min. Sequences of primers and probes used for DNA amplifications were like those reported by Yasunaga, et al¹⁶⁾. Primers used for amplification of TREC were 5'-TCCCTTTCAACCATGCTGA-

CA-3' and 5'-TGCCTATGCATCACCGTGC-3'. The probe was 5'-CTCTGGTTTTTGTAAAGGTGCC-CACTCCTG-3' labeled with fluorescent FAM at the 5' end and fluorescent TAMRA at the 3' end. To measure cell equivalents in the real-time PCR, recombination activating gene 1 (*RAG-1*) sequence in each sample was quantified by the method similar to that for TREC. The sequences of primers for *RAG-1* exon 2 detection were also similar to those reported by Yasunaga, et al¹⁶⁾: 5'-CCCACCTTGGGACTCAGTTCT-3' and 5'-CACCCGGAACAGCTTAAATTTTC-3', and the probe was 5'-CCCCAGATGAAATTCAGCACCCACATA-3' labeled with FAM (reporter) at the 5' end and TAMRA (quencher) at the 3' end. The crude DNA extracts (7 μ l) were mixed with 10 μ l of AbsoluteTM QPCR Mixes (Abgene House, Surrey, UK), and each 1 μ l of the primer (final concentration, 0.3 μ M) and probe (final concentration, 0.2 μ M) was added to the mixture. The PCR conditions were 50 cycles of 15 seconds at 95 °C followed by 60 seconds at 60 °C. All experiments were performed and analyzed by the ABI PRISM 7900 Sequence Detection Systems (Applied Biosystems, Foster City, CA). Number of TRECs in each sample was calculated using the following formula.

$$\begin{aligned} & \text{Number of TREC copies per 10,000 cells} \\ & = 10,000 / 2^{(\text{cycles required for the significant amplification of} \\ & \text{TREC}) - (\text{cycles required for the significant amplification of } RAG-1) - 1} \end{aligned}$$

Data analysis

A standard multiple-linear-regression method was used to regress log-transformed number of TRECs (per 10⁵ cells) on age of the individual at the time of the bombing (ATB), gender and DS02 A-bomb radiation exposure dose. The zero value was impossible of log transformation, and thus the value showing zero for the number of TREC copies per 10,000 cells was replaced with 0.05 when the value was transformed into natural log. All statistical analyses were carried out using the SAS program (SAS Institute Inc., Cary, NC, USA).

Results

Quantification of TRECs by real-time PCR

In our Institute, the amount of blood to collect from A-bomb survivors is limited so as to cause the least amount of anxiety in the donor. We therefore tried to directly

amplify TREC sequences by real-time PCR in crude DNA extracts from lymphocyte fractions that were treated with proteinase K to try to avoid loss of cellular DNA during its purification from a small number of blood cells as few as 10^5 . We similarly quantified *RAG-1* copies in each sample by the real-time PCR to measure cell equivalents in the crude extracts. Representative amplification profiles of crude DNA extracts from CD45RA⁺ naïve and

CD45⁻ memory CD4 T cell fractions isolated from the same individual are shown in Fig. 1. The number of PCR cycles required to give adequate amplification of TREC was much higher in the naïve CD4 T-cell fraction than in the memory CD4 T-cell fraction, whereas the number of cycles to give significant amplification of *RAG-1* was about equal in these T-cell fractions. Similarly, the number of TREC copies per 10,000 cells calculated from the

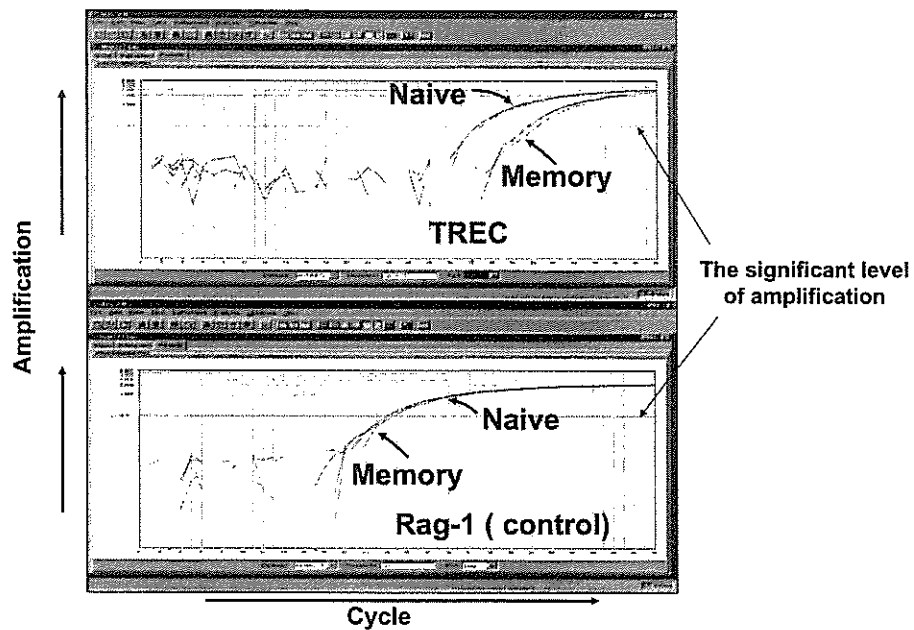


Fig.1 Representative amplification profiles in crude DNA extracts from CD45RA⁺ naïve and CD45⁻ memory CD4 T cell fractions isolated from a typical individual. The upper and lower panels show real-time PCR for the TREC and *RAG-1* sequences, respectively.

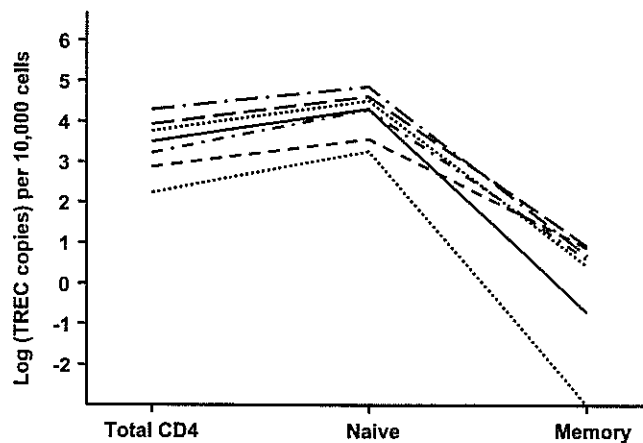


Fig. 2 The number of TREC copies per 10,000 cells in total CD4 T-cell fractions, and naïve and memory CD4 T-cell fractions from seven laboratory controls (five males aged 38-60, and two females aged 39 and 43). Each line indicates the value of the number of TREC copies in each individual.

difference between the cycles for TREC and *RAG-1* amplifications was much higher in the naïve CD4 T-cell fraction than in the memory CD4 T-cell fraction among seven laboratory volunteers (Fig. 2).

To determine whether the real-time PCR methods can quantitatively detect TRECs, we analyzed amplification profiles in samples containing a TREC-negative cell population and graded numbers of CD45RA⁺ naïve CD4 T cells that were obtained from a young adult and therefore were expected to contain large numbers of TRECs. As shown in Fig. 3, there was a reasonable linear correlation ($r = -0.95$, constant of proportion is -1.02) between the cycles and the number (base 2 logarithm) of naïve CD4

T cells, indicating that the two-fold reduction in the number of naïve CD4 T cells correspond to almost twice increase of the PCR cycle. Furthermore, reasonable reproducibility (coefficient values were 8.2, 18.3, and 21.8 in three individuals) were found in our real-time PCR analyses (Fig. 4). These results provided a basis to believe that the real-time PCR could accurately quantify the numbers of TREC copies in T-cell fractions obtained from A-bomb survivors or any other human population.

TREC analyses among A-bomb survivors

Thus far the numbers of TREC copies in CD4 T-cell fractions from 445 survivors and those in CD8 T-cell fractions from 426 survivors have been examined. Fig. 5

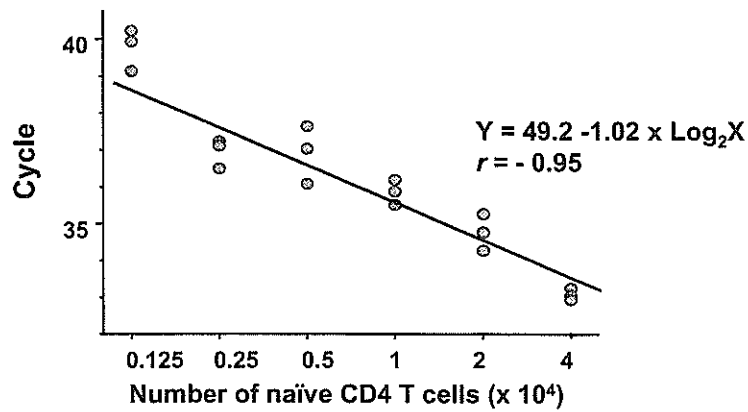


Fig. 3 The relationship between the number of cells containing TRECs and PCR cycles to give the significant amplification of TRECs. Each sample consisted of 10⁵ cells containing a TREC-negative cell population and the indicated number of CD45RA⁺ naïve CD4 T cells that were obtained from a young adult male. The TREC-negative cells were prepared from a T-cell line (KI-19) that was clonally propagated *in vitro* as described⁶⁾. We confirmed that these cells contain no detectable TREC in the real-time PCR.

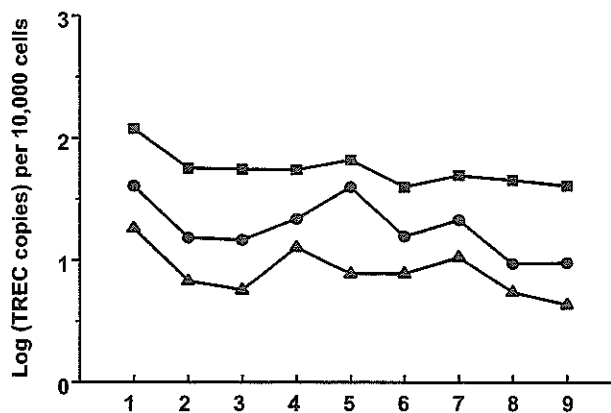


Fig. 4 Reproducibility in the real-time PCR analyses. Each 10⁵ peripheral blood mononuclear cells from three laboratory controls was stored at -20 °C and analyzed nine different times during about one and a half years. Each line indicates the value of each individual.

shows the relationships between the number of TREC copies in the CD4 or CD8 T-cell fraction and the age of the survivors at the time of the bombing (ATB). Although the points are widely scattered, the number of TREC copies significantly ($p < 0.001$) decreased with increase of age ATB in both the CD4 and CD8 T-cell fractions. The same kind of trend was observed when the values were analyzed using age of the survivors at the time of examination instead of age ATB (data not shown). As for the numbers of TREC copies in the CD4

T-cell fraction, however, the individual log-values were normally distributed in survivors who were age ATB < 20 but not when individuals with age ATB ≥ 20 were included. Whereas, no log-normal distribution could be observed as for the numbers of TREC copies in the CD8 T-cell fraction even when those who were age ATB ≥ 20 were excluded. This might be due to the fact that individuals who showed extremely low numbers of TREC copies in the CD4 T-cell fraction were mostly distributed in the age ATB ≥ 20 group while those who showed

Table 1 Multi-regression analysis of effects on the number of TREC copies in CD4 and CD8 T-cell fractions of A-bomb survivors (Age ATB < 20)*

Factors (unit)	% Change	95% CI**	<i>p</i>
CD4 (n = 313)			
Dose (1 Gy)	-14.8	-32, 2.4	0.09
Age (10 y)	-50.8	-27.1, -74.5	< 0.001
Gender (M:1, F:2)	77.2	48.3, 106	< 0.001
CD8 (n = 300)			
Dose (1 Gy)	-19.2	-49.8, 11.4	0.2
Age (10 y)	-74.4	-31.8, -117	< 0.001
Gender (M:1, F:2)	287	235, 339	< 0.001

*Associations of the number of TREC copies with age at the time of bombing (age ATB), gender, and radiation dose (dose) were analyzed based on a multiple regression model.

**CI = confidence interval

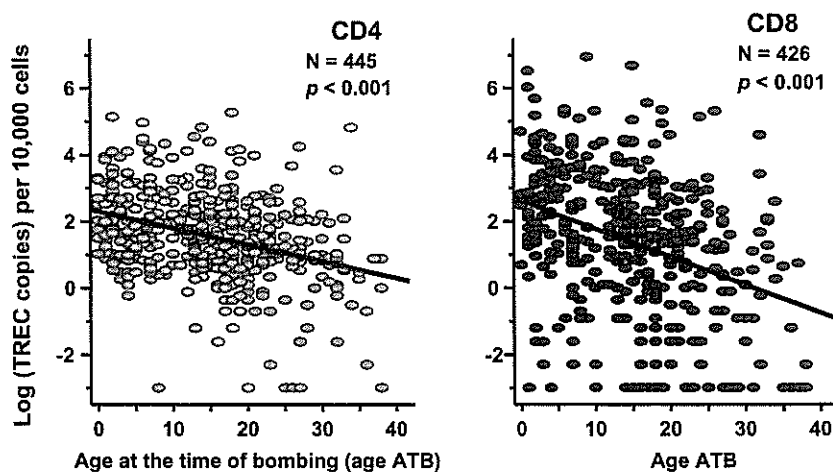


Fig. 5 The number of TREC copies in the CD4 (left panel) or CD8 (right panel) T-cell fraction in each individual is plotted against the age of individual at the time of the bombing (ATB). Each line denotes the regression between the number of TREC copies and age ATB.

extremely low numbers of TREC copies in the CD8 T-cell fraction appeared in both younger and older age ATB groups (Fig. 5). There was a strong correlation ($r = 0.7$) between the numbers of TREC copies in the CD4 and CD8 T-cell fractions from the same survivors who were age ATB < 20, indicating that individual ability of thymic CD4 T-cell production may be somewhat proportional to that of thymic CD8 T-cell production at least in the age ATB < 20 group.

A multiple regression analysis was conducted for the number of TREC copies in the CD4 or CD8 T-cell fraction among survivors who were age less than 20 ATB, because the individual TREC number in this group appeared to be close to the normal distribution (especially in the CD4 T-cell fraction) and to be strongly affected by age ATB or gender. The results are summarized in Table 1. The number of TREC copies in the CD4 T-cell fraction decreased significantly with age ATB ($p < 0.001$) and was higher in females than in males ($p < 0.001$). These data also suggested that there might be a dose-dependent decrease in the number of TRECs in the CD4 T-cell fraction of the survivors ($p = 0.09$). Similar statistically significant trend for age ATB ($p < 0.001$) and gender difference ($p < 0.001$) were observed in the CD8 T-cell fraction of the survivors. The number of TRECs in the CD8 T-cell fraction of the survivors appeared to decrease somewhat with radiation dose, but this dose trend was not statistically significant ($p = 0.2$).

Discussion

Our present study suggests that the numbers of TREC copies in both CD4 and CD8 T-cell fractions decrease with age. TREC copy number is higher in females than in males. We believe this to be the first report of gender difference in TREC copy number in a human population. Because our study population consisted of persons aged over 58 years, it is likely that age-dependent decline in human thymic output represents a characteristic of aging among the elderly. Because thymic involution resulting in reduction of cellularity in this organ is known to be a primary cause of age-dependent decline in TREC copy numbers in both CD4 and CD8 T-cell populations¹⁷⁾, the present results suggest that thymus involution may continue even after age 58. The observed gender difference

as these populations age suggests that the aging process differently affects thymic involution in males and females. A further analysis including younger subjects is needed to test this hypothesis.

Our previous studies^{7, 8, 15)} indicated that the size of naïve cell pools in CD4 T-cell populations was reduced possibly as a consequence of radiation exposure among A-bomb survivors. One of the most plausible mechanisms for size reduction of naïve T-cell populations could have resulted from insufficient supply of new T cells from the thymus, since the majority of naïve T cells develop in the thymus. We therefore expected to find similar reduction in number of recent thymic emigrant cells in our latest study population. Even though the current study is preliminary and radiation effect was suggested only among survivors who were age < 20 years ATB, the result for number of TREC copies in CD4 T-cell populations supports the possibility that A-bomb radiation exposure can induce long-term impairment of CD4 T-cell production. Actually, number of TREC copies appeared to positively correlate ($p < 0.001$, $r = 0.3$) with proportion of CD45RA⁺ naïve cells in the CD4 T-cell population among the 443 survivors available for examination for both TREC number and CD45RA expression in their CD4 T-cell populations (data not shown). Therefore, it is reasonable to assume that radiation-induced reduction in production of new CD4 T cells in the thymus could cause impaired maintenance of naïve CD4 T-cell pools among radiation-exposed individuals.

It has been reported¹⁴⁾ that significantly fewer CD4 T cells containing TRECs are seen in bone marrow transplantation patients exposed to whole-body irradiation more than 20 years ago, even though the doses (10 Gy or more) far exceeded those received by A-bomb survivors. Because reconstituted hematopoietic cell populations of such patients are almost entirely derived from unirradiated donors, and with their own thymus epithelial cells severely irradiated, reduction in number of TREC copies may be due to radiation effect on the ability of thymus epithelial cells to support thymopoiesis. In an earlier study⁵⁾ using mouse models, it was shown that there are radiation-dose-dependent decreases in T-cell regeneration activity in mice subjected to thymectomy followed

by transplantation with irradiated thymuses and in those that underwent local thymic irradiation. Effects of irradiation on mice undergoing bone marrow transplantation³⁾ are also noted for dose-dependent reductions in the production of IL-7, which is essential for T-cell development, and in the number of MHC class II⁺ epithelial cells, which are the primary source of IL-7. It is therefore hypothesized that A-bomb radiation damaged thymic stroma, in which epithelial cells primarily support thymopoiesis, and induced long-term impairment in the ability of the thymus to supply new T cells containing TREC_s into the periphery.

Another hypothesis to be tested is that reduction of TREC copy number in the CD4 T-cell populations of A-bomb survivors might have resulted from dilution of TREC-bearing cell populations by homeostatic and/or antigenic proliferations of naïve T-cell populations followed by their transfer to memory T-cell pools. It is known that such proliferations of naïve T cells are largely dependent on their interaction with dendritic cells⁴⁾. We are planning to evaluate the *in vivo* cell division frequencies of both naïve and memory CD4 T-cell populations by analyzing telomere lengths in these T-cell populations among A-bomb survivors. We will also explore a potentially valuable method for analyzing dendritic-cell reconstitution following T-cell depletion by radiation.

Despite that similar mechanisms are plausible for the size reduction of naïve CD8 T-cell populations that we reported among A-bomb survivors¹⁵⁾, we did not observe in the present study any statistically significant or even suggestive association between numbers of TREC copies in CD8 T-cell populations and radiation dose. This could reflect that the effect of aging and/or gender on TREC counts is more pronounced in CD8 T-cell populations than in CD4 T-cell populations (Table 1), which would obscure the effect of radiation *per se* on CD8 T-cell populations among elderly survivors. We also noted that the proportion of naïve CD8 T cells in peripheral blood lymphocyte populations was as low as a few percent, whereas that of naïve CD4 T cells ordinarily exceeds 10 percent among our study's elderly survivor population¹⁵⁾. Thus, it is expected that naïve CD8 T cells containing TREC in T-cell fractions we analyzed are very infrequent when

compared with naïve CD4 T cells containing TREC. More sophisticated statistical analyses with additional samples will be necessary to evaluate possible radiation effects on such a small number of cells per sample. Such an approach would also provide improved evidence regarding possible long-term effects of radiation exposure on the human T-cell system involving both CD4 and CD8 T-cell populations.

Acknowledgements

The authors are grateful to Drs. Tomonori Hayashi, Seishi Kyoizumi Kei Nakachi and Charles A. Waldren for their helpful discussions. We also would like to thank Mika Yonezawa and Yoko Takemoto for their manuscript preparation.

The Radiation Effects Research Foundation (RERF), Hiroshima and Nagasaki, is a private nonprofit foundation funded by the Japanese Ministry of Health, Labour and Welfare (MHLW) and the United States Department of Energy (DOE) the latter through the National Academy of Sciences. This publication was based on RERF Research Protocol RP 4-02 and supported in part by Grants-in-Aid for Scientific Research from the Ministry of Education, Culture, Sports, Science, and Technology of Japan and the MHLW.

References

- 1) Douek DC, McFarland RD, Keiser PH, et al: Changes in thymic function with age and during the treatment of HIV infection. *Nature* 396:690-695, 1998
- 2) Douek DC, Vescio RA, Betts MR, et al: Assessment of thymic output in adults after haematopoietic stem-cell transplantation and prediction of T-cell reconstitution. *Lancet* 355:1875-1881, 2000
- 3) Chung B, Barbara-Burnham L, Barsky L, et al: Radiosensitivity of thymic interleukin-7 production and thymopoiesis after bone marrow transplantation. *Blood* 98:1601-1606, 2001
- 4) Fry TJ, Sinha M, Milliron M, Chu YW, et al: Flt3 ligand enhances thymic-dependent and thymic-independent immune reconstitution. *Blood* 104:2794-2800, 2004
- 5) Hirokawa K, Sado T: Radiation effects on regeneration and T-cell-inducing function of the thymus. *Cell*.

- Immunol. 84:372-379. 1984
- 6) Kusunoki Y, Kodama Y, Hirai Y, et al: Cytogenetic and immunologic identification of clonal expansion of stem cells into T and B lymphocytes in one Atomic-bomb survivor. *Blood* 86: 2106-2112, 1995
 - 7) Kusunoki Y, Kyoizumi S, Hirai Y, et al: Flow cytometry measurements of subsets of T, B and NK cells in peripheral blood lymphocytes of atomic bomb survivors. *Radiat. Res.* 150: 227-236, 1998
 - 8) Kusunoki Y, Yamaoka M, Kasagi F, et al: T cells of atomic bomb survivors respond poorly to stimulation by *Staphylococcus aureus* toxins in vitro: does this stem from their peripheral lymphocyte populations having a diminished naive CD4 T-cell content? *Radiat. Res.* 158: 715-724, 2002
 - 9) Mackall CL, Hakim FT, Gress RE: T-cell regeneration: all repertoires are not created equal. *Immunol. Today* 18:245-251, 1997
 - 10) McFarland RD, Douek DC, Koup RA, et al: Identification of a human recent thymic emigrant phenotype. *Proc. Natl. Acad. Sci. U. S. A.* 97: 4215-4520, 2000
 - 11) Miller RA: The aging immune system: primer and prospectus. *Science* 273:70-74, 1996
 - 12) Preston DL, Pierce DA, Shimizu Y, et al: Effect of recent changes in atomic bomb survivor dosimetry on cancer mortality risk estimates. *Radiat. Res.* 162:377-389, 2004
 - 13) Verschuren MC, Wolvers-Tettero IL, Breit TM, et al: Preferential rearrangements of the T cell receptor-delta-deleting elements in human T cells. *J. Immunol.* 158:1208-1216, 1997
 - 14) Weinberg K, Blazar BR, Wagner JE, et al: Factors affecting thymic function after allogeneic hematopoietic stem cell transplantation. *Blood* 97:1458-1466, 2001
 - 15) Yamaoka M, Kusunoki Y, Kasagi F, et al: Decreases in percentages of naive CD4 and CD8 T cells and increases in percentages of memory CD8 T-cell subsets in the peripheral blood lymphocyte populations of A-bomb survivors. *Radiat. Res.* 161:290-298, 2004
 - 16) Yasunaga J, Sakai T, Nosaka K, et al: Impaired production of naive T lymphocytes in human T-cell leukemia virus type I-infected individuals: its implications in the immunodeficient state. *Blood* 97: 3177-3183, 2001
 - 17) Ye P, Kirschner DE: Reevaluation of T Cell Receptor Excision Circles as a Measure of Human Recent Thymic Emigrants. *J.Immunol.* 168: 4968-4979, 2002

Corresponding author: Yoichiro Kusunoki, Ph.D.

Department of Radiobiology/Molecular Epidemiology, Radiation Effects Research Foundation,
5-2 Hijiyama Park, Minami-ku, Hiroshima, 732-0815 Japan
Phone: 082-261-3131, Fax: 082-261-3170, E-mail: ykusunok@rerf.or.jp

別冊請求先：〒732-0815 広島市南区比治山公園 5-2 放射線影響研究所放射線生物学/分子疫学部 楠洋一郎
Tel: (082)261-3131, Fax: (082)261-3170, E-mail: ykusunok@rerf.or.jp

Role of Single-stranded DNA in Targeting REV1 to Primer Termini*[§]

Received for publication, March 29, 2006, and in revised form, June 21, 2006. Published, JBC Papers in Press, June 27, 2006, DOI 10.1074/jbc.M602967200

Yuji Masuda and Kenji Kamiya¹

From the Research Institute for Radiation Biology and Medicine, Hiroshima University, Hiroshima 734-8553, Japan

Cellular functions of the *REV1* gene have been conserved in evolution and appear important for maintaining genetic integrity through translesion DNA synthesis. This study documents a novel biochemical activity of human REV1 protein, due to higher affinity for single-stranded DNA (ssDNA) than the primer terminus. Preferential binding to long ssDNA regions of the template strand means that REV1 is targeted specifically to the included primer termini, a property not shared by other DNA polymerases, including human DNA polymerases α , β , and η . Furthermore, a mutant REV1 lacking N- and C-terminal domains, but catalytically active, lost this function, indicating that control is not due to the catalytic core. The novel activity of REV1 protein might imply a role for ssDNA in the regulation of translesion DNA synthesis.

The majority of both spontaneous and DNA damage-induced mutations in eukaryotes results from replication processes in which REV1, REV3, and REV7 proteins play major roles. Studies of *REV* genes originated with the isolation of yeast *rev* mutants (1, 2), which exhibited a reduced frequency of mutations following treatment with a variety of DNA-damaging agents (3). Deoxycytidyltransferase activity of the REV1 protein and DNA polymerase activity of the REV3-REV7 complex for translesion DNA synthesis were discovered in the pioneering work of Lawrence and co-workers (4, 5). By using information obtained from yeast studies, homologues of the encoding genes were subsequently identified in mammals (6–13), and it is now well established that the pathway has been conserved in evolution from the yeast to humans.

REV1 is a member of the Y family of DNA polymerases, which also includes DNA polymerase (pol)² IV and V in *Escherichia coli*, and DNA pol η , ι , and κ in eukaryotes (14, 15). These proteins are required for translesion DNA synthesis because many lesions block typical replicative DNA polymerases. How-

ever, the REV1 protein almost exclusively utilizes only dCTP, in contrast to the other members of the family, and preferentially inserts dCMP opposite template G and a variety of damaged bases and apurinic/apyrimidinic sites (4, 6, 7, 11, 16–18). Because of this preference, REV1 has been called a deoxycytidyltransferase (3, 4). This novel activity has been maintained throughout eukaryotic evolution, implying a contribution to survival (3). Recently, it was demonstrated that the specificity for dCMP is tightly regulated by formation of hydrogen bonds with an arginine residue in the protein, but not template G (19). Indeed, dCMP residues are known to be incorporated opposite apurinic/apyrimidinic sites in the majority of bypass events in wild type yeast cells but not the *rev1* Δ strain (20–23).

A second function of the *REV1* gene product in the mutagenesis pathway has also been proposed, independent of its action as a deoxycytidyltransferase (24). Methyl methanesulfonate-induced mutagenesis has been shown to be normal in a site-directed mutant lacking deoxycytidyltransferase activity (25). Furthermore, although the REV1 protein does not allow bypass of thymine-thymine (6-4) photoproducts *in vitro*, the gene is required for bypass replication of this lesion in yeast cells (24, 26, 27). With respect to the second function, the BRCA1 C-terminal domain of REV1 has an essential function, mutation abolishing UV-induced mutagenesis, even if the protein retains normal levels of transferase activity *in vitro* (24, 27).

Evolutionary preservation of functions of the mammalian *REV1* gene was first indicated by the finding that human cell lines expressing high levels of human *REV1* antisense RNA exhibit a much reduced frequency of 6-thioguanine-resistant mutants induced by UV light (10). This feature was confirmed in another experimental system using a ribozyme that cleaves human *REV1* mRNA (28) and with an RNA interference down-regulating mouse Rev1 function (29). Furthermore, mouse embryonic stem cells carrying a mutation lacking the BRCA1 C-terminal domain of the *Rev1* gene also exhibit sensitivity to a wide range of DNA-damaging agents and a reduced level of UV light-induced mutations (30, 31). Recently, chicken $\Delta Rev1$ -DT40 cell lines were generated and found to exhibit slow growth and sensitivity to a wide range of DNA-damaging agents (32–34).

Although studies of the cellular functions of the *REV1* gene in yeast to humans have shed light on its importance for maintaining genetic integrity, the biochemical basis is poorly understood. It is known that both mouse and human REV1 proteins interact with REV7 and other Y family polymerases through the same C-terminal region (35–38). In particular, the REV1-REV7 interaction is very stable and results in formation of a heterodimer in yeast and humans (39, 40). The C-terminal region

* This work was supported by grants from the Ministry of Education, Culture, Sports, Science, and Technology of Japan (to Y. M. and K. K.) and by the 21st Century Center of Excellence Program from the Ministry of Education, Culture, Sports, Science and Technology of Japan (to K. K.). The costs of publication of this article were defrayed in part by the payment of page charges. This article must therefore be hereby marked "advertisement" in accordance with 18 U.S.C. Section 1734 solely to indicate this fact.

[§] The on-line version of this article (available at <http://www.jbc.org>) contains supplemental Fig. S1.

¹ To whom correspondence should be addressed: Research Institute for Radiation Biology and Medicine, Hiroshima University, 1-2-3 Kasumi, Minami-ku, Hiroshima 734-8553, Japan. Tel.: 81-82-257-5842; Fax: 81-82-257-5844; E-mail: kkamiya@hiroshima-u.ac.jp.

² The abbreviations used are: pol, DNA polymerase; ssDNA, single-stranded DNA; BSA, bovine serum albumin.

of yeast Rev1 is also required for stimulation of yeast pol ζ (41), although the amino acid sequence is not conserved. From these observations, a noncatalytic role in translesion DNA synthesis has been proposed (35–41).

In this report, we document a novel biochemical property of human REV1. We show that REV1 has single-stranded DNA (ssDNA) binding activity with affinity much higher than that of the primer-template. After binding to ssDNA, REV1 can translocate and be targeted to primer termini. We consider that this property might reflect a particular biochemical function required for regulation of the repair pathway involved in lesion bypass replication.

EXPERIMENTAL PROCEDURES

Oligonucleotides—The oligonucleotide sequences were as follows: H1, 5'-GACGCTGCCGAATTCTGGCTTGCTAGGACATCTTTGCCACGTTGACCCG-3'; H2, 5'-CGGGTCAACGTGGGCAAAGATGTCCTAGCAATGTAATCGTCTATGACGTC-3'; H3, 5'-GACGTCATAGACGATTACATTGCTAGGACATGCTGTCTAGAGACTATCGC-3'; and H4, 5'-GCGATAGTCTCTAGACAGCATGTCCTAGCAAGCCAGAAATTCGGCAGCGTC-3'. The primer-template, P5786T, was made by annealing the 5'-³²P-labeled primer P5786 (5'-GTC-TACAAGTTCAC-3') with the template 5786T (5'-ATTCTG-AGCAGCCCGGATGGTGAACCTTGTAGAC-3'). Others are shown in Fig. 3A.

Plasmids—Human *POLB* cDNA was amplified from HeLa cDNA by PCR and inserted into the NdeI-BamHI site of a pET20b(+) vector (Novagen) to yield plasmid pET-POLB. Human *POLH* cDNA was amplified by PCR from a plasmid carrying human *POLH* cDNA, kindly provided by Dr. F. Hanaoka, Osaka University, Osaka, Japan (42), and inserted into the NdeI-BamHI site of a pET15b vector (Novagen) to yield pET-h6-POLH. Human *POLA* cDNA was amplified by PCR from a plasmid carrying human *POLA* cDNA, kindly provided by Dr. M. Suzuki, Nagoya University, Nagoya, Japan (43), and inserted into the NdeI-XhoI site of a pET15b vector (Novagen) to yield pET-h6-POLA. Human *POLA2* cDNA was amplified from HeLa cDNA by PCR and inserted into the NdeI-KpnI site of a pCDFK vector, which was made by deletion of an EcoNI-AflIII fragment and replacement of the streptomycin resistance gene of pCDFDuetTM-1 (Novagen) with the kanamycin resistance gene from pSY343 (44), to yield pCDFK-POLA2. The nucleotide sequences were verified in all these plasmids.

Proteins—Intact REV1 was purified as described (17), along with mutants (6). Human pol β was overproduced in BL21 (DE3) (45) harboring pET-POLB and similarly purified (46).

His-tagged human pol η (h6-pol η) was purified from overexpressing *E. coli* cells as follows. BL21 (DE3) (45) harboring pET-h6-POLH was grown in 500 ml of LB medium supplemented with ampicillin (250 mg/ml) at 15 °C with aeration until the culture reached an A_{600} value of 0.6. Isopropyl β -D-thiogalactopyranoside was added to 0.2 mM, and incubation was continued for 10 h. The resultant cell paste was resuspended in 2 ml of buffer I (50 mM HEPES-NaOH, pH 7.5, 0.1 mM EDTA, 10 mM β -mercaptoethanol) containing 1 M NaCl per 1 g of cells and frozen in liquid nitrogen. The cells were thawed in ice water and lysed after addition of phenylmethylsulfonyl fluoride to 0.1 mM

by introduction of 100 mM spermidine and 4 mg/ml lysozyme in buffer I containing 1 M NaCl, to 10 mM and 0.4 mg/ml, respectively. The cells were incubated on ice for 30 min, heated in a 37 °C water bath for 2 min, and further incubated on ice for 30 min at 4 °C. Then the lysate was clarified by centrifugation at 85,000 \times g for 30 min at 4 °C. Subsequent column chromatography was carried out at 4 °C using a fast protein liquid chromatography system (GE Healthcare). After adding imidazole to 50 mM, the lysate was applied at 0.1 ml/min to a 1-ml HiTrap chelating column (GE Healthcare), which had been treated with 0.1 M NiSO₄ and then equilibrated with buffer A (50 mM HEPES-NaOH, pH 7.5, 10 mM β -mercaptoethanol, 10% glycerol) containing 1 M NaCl and 50 mM imidazole. The column was washed with 10 ml of equilibration buffer, and then 10 ml of buffer A containing 1 M NaCl and 100 mM imidazole, and the h6-pol η was eluted with 10 ml of a linear gradient of 100–300 mM imidazole in buffer A containing 1 M NaCl. Fractions containing the enzyme were pooled and concentrated and then loaded at 0.1 ml/min onto a Superdex 200 HR 10/30 column (GE Healthcare) equilibrated with buffer A containing 1 M NaCl. The h6-pol η peak fractions were pooled, frozen in liquid nitrogen, and stored at –80 °C.

His-tagged human pol α p180 (h6-p180) was purified as a complex with p70 from overexpressing *E. coli* cells. BL21 (DE3) (45) harboring both pET-h6-POLA and pCDFK-POLA2 was grown in 10 liters of "terrific" broth (47) supplemented with ampicillin (250 mg/ml) at 15 °C with aeration until the culture reached an A_{600} value of 0.6. Isopropyl β -D-thiogalactopyranoside was added to 0.2 mM, and the incubation was continued for 5 h. The resultant cell paste was resuspended in 2 ml of buffer I containing 0.5 M NaCl per 1 g of cells and frozen in liquid nitrogen. The cells were thawed in ice water and lysed after addition of phenylmethylsulfonyl fluoride to 0.1 mM by introduction of 100 mM spermidine and 4 mg/ml lysozyme in buffer I containing 0.5 M NaCl, to 10 mM and 0.4 mg/ml, respectively. The cells were incubated on ice for 30 min, heated in a 37 °C water bath for 2 min, and further incubated on ice for 30 min at 4 °C. Then the lysate was clarified by centrifugation at 85,000 \times g for 30 min at 4 °C. Subsequent column chromatography was carried out at 4 °C using a fast protein liquid chromatography system. After adding imidazole to 50 mM, the lysate was applied at 0.5 ml/min to a 1-ml HiTrap chelating column, which had been treated with 0.1 M NiSO₄ and then equilibrated with buffer A containing 0.5 M NaCl and 50 mM imidazole. The column was washed with 10 ml of equilibration buffer at 0.1 ml/min and then eluted with 10 ml of a linear gradient of 50–100 mM imidazole in buffer A containing 0.5 M NaCl. Fractions containing h6-p180-p70 were pooled, diluted with buffer A to 100 mM of NaCl, and applied at 0.1 ml/min to a 1-ml HiTrap Q HP column (GE Healthcare) equilibrated with buffer A containing 100 mM NaCl. The column was washed with 10 ml of equilibration buffer, and the h6-p180-p70 complex was eluted with 10 ml of a linear gradient of 100–500 mM NaCl in buffer A. Fractions containing h6-p180-p70 were pooled and loaded at 0.1 ml/min onto a Superose 6 HR 10/30 column (GE Healthcare) equilibrated with buffer A containing 0.5 M NaCl. The h6-p180-p70 peak fractions were pooled, frozen in liquid nitrogen, and

Targeting REV1 by Single-stranded DNA

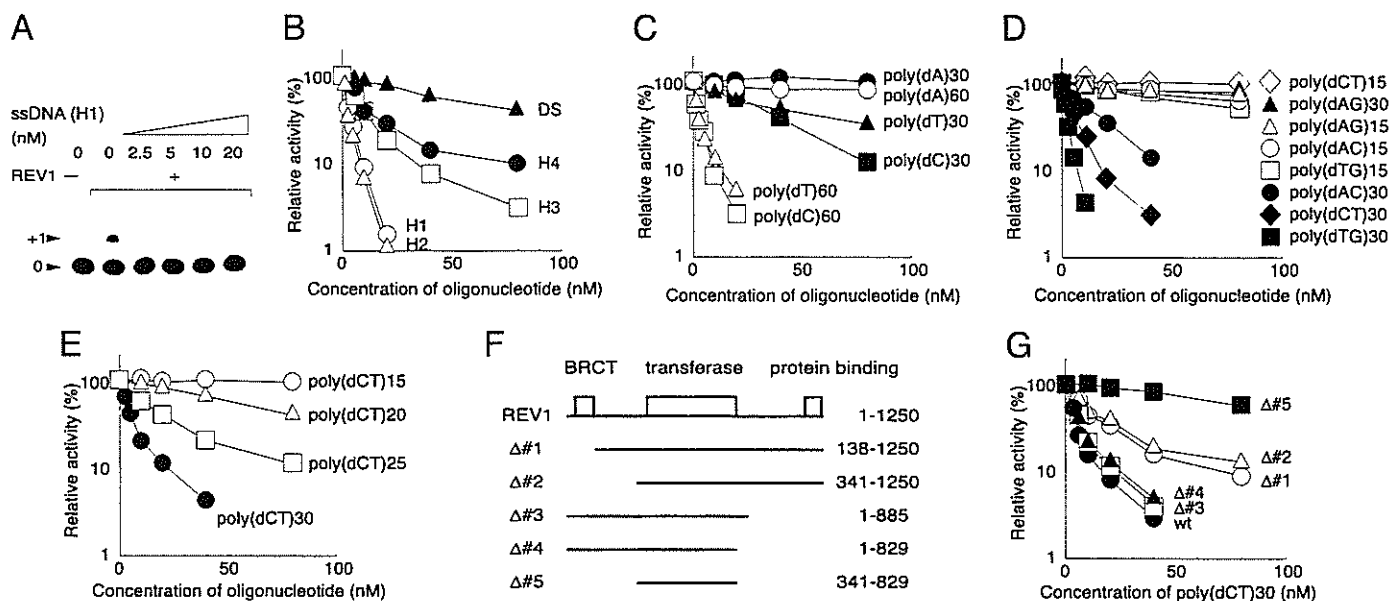


FIGURE 1. Inhibition of dCMP transferase activity of human REV1 protein by ssDNA. Inhibition of dCMP transferase activity of the REV1 protein (A–E) or its deletion derivatives (G) by various oligonucleotides is shown. Ten ng of REV1 or deletion derivatives (except for 5 ng of $\Delta 5$) and the primer-temple, P5786T (100 nM), were incubated under standard reaction conditions in the presence of the indicated concentration of oligonucleotides. The double-stranded DNA represented as *DS* in *B* was made by annealing H3 and the complementary oligonucleotide. The reaction products were resolved on 20% polyacrylamide gels containing 8 M urea and autoradiographed at -80°C (A, 0 and +1 represent positions of substrate and product, respectively), and the amounts of DNA present in each band were quantified (B–E and G). F, schematic representation of deletion mutants. The molar concentration of REV1 in the reactions was 2.8 nM and those of mutant REV1 were 3.1 nM $\Delta 1$, 3.8 nM $\Delta 2$, 3.9 nM $\Delta 3$, 4.2 nM $\Delta 4$, and 3.6 nM $\Delta 5$.

stored at -80°C . Protein concentrations were determined by protein assay using BSA (Bio-Rad) as the standard.

Primer Extension Assay—The primers were labeled using polynucleotide kinase (New England Biolabs) and $[\gamma\text{-}^{32}\text{P}]\text{ATP}$ (GE Healthcare) and annealed to the respective templates. The standard reaction mixture (25 μl) contained 50 mM Tris-HCl buffer, pH 8.0, 2 mM MgCl_2 , 0.1 mg/ml BSA, 5 mM dithiothreitol, 0.1 mM dCTP, 100 nM primer-temple, and 1 μl of protein sample diluted with buffer (50 mM HEPES-NaOH, pH 7.5, 500 mM NaCl, 10 mM β -mercaptoethanol, 10% glycerol, 0.1 mg/ml BSA) as indicated. After incubation at 30°C for 10 min, reactions were terminated with 10 μl of stop solution (30 mM EDTA, 94% formamide, 0.05% bromphenol blue, 0.05% xylene cyanol), and products were resolved on 20% polyacrylamide gels containing 8 M urea and autoradiographed at -80°C . The amount of DNA present in each band was quantified using a Bio-Imaging Analyzer BAS2000 (Fuji Photo Film Co., Ltd.). The conditions for the primer extension assay for DNA polymerase shown in Fig. 4B were identical to those for the dCMP transferase assay.

DNA Polymerase Assay—DNA polymerase activities shown in Fig. 4A were measured by incorporation of $[\alpha\text{-}^{32}\text{P}]\text{dCMP}$ using the unlabeled primer-temple, P5786T, as a substrate. The reaction mixture (25 μl) contained 50 mM Tris-HCl buffer, pH 8.0, 2 mM MgCl_2 , 0.1 mg/ml BSA, 5 mM dithiothreitol, 0.1 mM each of dGTP, dATP, dTTP, and $[\alpha\text{-}^{32}\text{P}]\text{dCTP}$ (GE Healthcare), 100 nM primer-temple (P5786T), and 1 μl of protein sample diluted with buffer (50 mM HEPES-NaOH, pH 7.5, 500 mM NaCl, 10 mM β -mercaptoethanol, 10% glycerol, 0.1 mg/ml BSA) as indicated. Ten ng of REV1, 3 ng of pol α , 2 ng of pol β , and 10 ng of pol η were used in 25- μl reaction mixtures. After incubation at 30°C for 10 min, reactions were terminated with

10 μl of 30 mM EDTA, and then 1- μl samples were spotted on DE81 paper (Whatman), which was washed three times with 0.5 M Na_2HPO_4 . The amount of incorporated $[\alpha\text{-}^{32}\text{P}]\text{dCMP}$ was determined as the radioactivity retained on the paper (48) and quantified using a Bio-Imaging Analyzer BAS2000 (Fuji Photo Film Co., Ltd.).

Electrophoretic Mobility Shift Assay—Poly[d(C-T)] oligonucleotides with various lengths were labeled using polynucleotide kinase (New England Biolabs) and $[\gamma\text{-}^{32}\text{P}]\text{ATP}$ (GE Healthcare). Assays of DNA binding were performed with modification of a method described previously (6). Reaction mixtures (10 μl) contained 50 mM Tris-HCl buffer, pH 8.0, 2 mM MgCl_2 , 0.2 mg/ml BSA, 5 mM dithiothreitol, 0.1 mM dCTP, 50 μM oligonucleotide, and 1 μl of protein sample diluted with buffer (50 mM HEPES-NaOH, pH 7.5, 500 mM NaCl, 10 mM β -mercaptoethanol, 10% glycerol, 0.1 mg/ml BSA) as indicated. Incubation was on ice for 20 min followed by loading on pre-running 4% polyacrylamide gels (79:1 acrylamide/bisacrylamide). The electrophoresis buffer contained 6 mM Tris-HCl, pH 7.5, 5 mM sodium acetate, and 0.1 mM EDTA, and the gels were subjected to a constant voltage of 8 V/cm for 2 h at 6°C . Following gel electrophoresis, the gels were dried and autoradiographed at -80°C .

RESULTS

High Affinity Binding of REV1 to ssDNA—During biochemical characterization of the dCMP transferase reactions of human REV1 protein, we found a synthetic oligonucleotide, H1, to be a strong inhibitor of the transferase activity of the REV1 (Fig. 1A). In reactions containing 100 nM primer-temple and 2.8 nM REV1, the transferase activity dropped to less than 10% in the presence of 10 nM of the H1 (Fig. 1, A and B). To

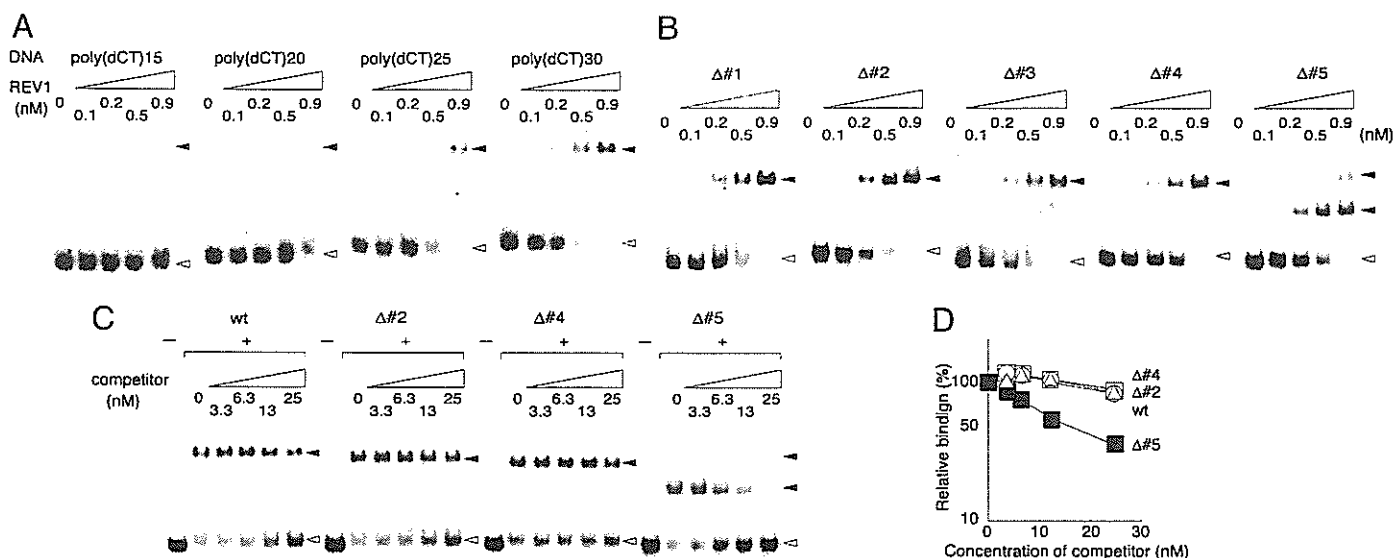


FIGURE 2. Analysis by electrophoretic mobility shift assay of ssDNA binding to the REV1 protein. *A* and *B*, electrophoretic mobility shift assays of ssDNA binding to REV1 (*A*) and its deletion derivatives (*B*). Poly[d(C-T)] consisting of the indicated repeats (*A*) or d(C-T)₃₀ 60-mer (*B*) were incubated with REV1 or deletion mutants at the indicated concentrations. Filled and open arrowheads indicate the positions of the DNA-REV1 complex and the free DNA, respectively. *C*, competition assay of REV1-ssDNA binding activity. In binding reactions with 0.9 nM of REV1 or deletion derivatives, the indicated concentrations of unlabeled primer-template, P5786T, were incubated as a competitor. *D*, quantified results of *C*.

ascertain whether the inhibitory effect was because of a specific nucleotide sequence, oligonucleotides of different sequences (H2–H4) were tested (Fig. 1*B*). The results suggested that the inhibitory effect was not because of a specific nucleotide sequence, although each oligonucleotide exhibited a different extent of inhibition. When the oligonucleotide was annealed with the complementary oligonucleotide and converted to double-stranded DNA, such an effect was much decreased (Fig. 1*B*). The remaining effect might be due to trace contamination of ssDNA (data not shown). To exclude the possibility that the effect is due to local secondary structures formed by the oligonucleotides, we tested 30- and 60-mer oligonucleotides composed of one or two nucleotides, which are guaranteed not to form secondary structures (Fig. 1, *C* and *D*). The results revealed general features for the inhibition. First, it was not because of secondary structures of the oligonucleotides. Second, the composition of the nucleotides affected the extent of inhibition, whereas polypurines, poly(dA) and poly[d(A-G)], showed no effect. Third, the extent of inhibition was stronger with 60- than 30-mer oligonucleotides with the same composition of nucleotides. Furthermore, we systematically addressed the effect of the length using poly[d(C-T)] as a model oligonucleotide (Fig. 1*E*) and found the extent of inhibition to correlate synergistically with the length. In a control experiment, we demonstrated that REV1 could not transfer dCMP to the 3' end of the d(C-T)₃₀, 60-mer oligonucleotide, under those reaction conditions (supplemental Fig. 1), indicating that the inhibition is not because of random priming reactions with the oligonucleotide. In following experiments, we used poly[d(C-T)] oligonucleotides as model ssDNA substrates.

The inhibitory effect might be due to high affinity binding of the REV1 to the ssDNA, and consequently, it should compete with the primer-template. To examine REV1 ssDNA binding activity, we performed gel mobility shift assays using poly[d(C-T)] oligonucleotides with various lengths as substrates and

detected REV1-ssDNA complexes (Fig. 2*A*). When we tested the d(C-T)₁₅, 30-mer oligonucleotide, as a substrate, no complexes could be detected. However, when the length was increased, complexes became visible and were stable. The apparent affinity of REV1 for the oligonucleotides proved to be relative to their lengths. On the 60-mer oligonucleotide, the apparent affinity was very high with less than 1 nM of estimated K_d . Most importantly, the degree of apparent affinity of REV1 for the oligonucleotides of various lengths showed good agreement with the degrees of their inhibitory effects on transferase activity (Fig. 1*E*).

Analysis of Truncated REV1 Proteins—Next, we examined the properties of truncated REV1 proteins (Δ1–Δ5) (Fig. 1*F*) with intact transferase activity (Fig. 3*E*, panel *a*). First, the inhibitory effects of 60-mer poly[d(C-T)] were examined (Fig. 1*G*). The effect of truncation of the C-terminal Δ3 and Δ4 was the same as observed with the full-length protein. On the other hand, truncation of the N-terminal Δ1 and Δ2 resulted in partial resistance to ssDNA. However, truncation of both N- and C-terminal Δ5 showed a much greater effect. The activity of the mutant protein Δ5 consisting of only the transferase domain was not inhibited by the oligonucleotide, indicating inhibition by ssDNA to be modulated by domains outside the transferase domain of REV1.

Then we tested ssDNA binding activity of the mutants (Fig. 2*B*). Surprisingly, binding of the 60-mer poly[d(C-T)] to all the truncated proteins was essentially identical to that to full-length REV1 (Fig. 2*B*). With the full-length REV1, the transferase activity could be inhibited by ssDNA binding. However, this was not the case with truncated protein Δ5. Therefore, we addressed the question of whether the primer-template is accessible to REV1-ssDNA complexes (Fig. 2, *C* and *D*). If REV1 could interact with a primer-template after forming a complex with ssDNA, the complex would be sensitive to an addition of a large amount of the primer-template. In the REV1-ssDNA

Targeting REV1 by Single-stranded DNA

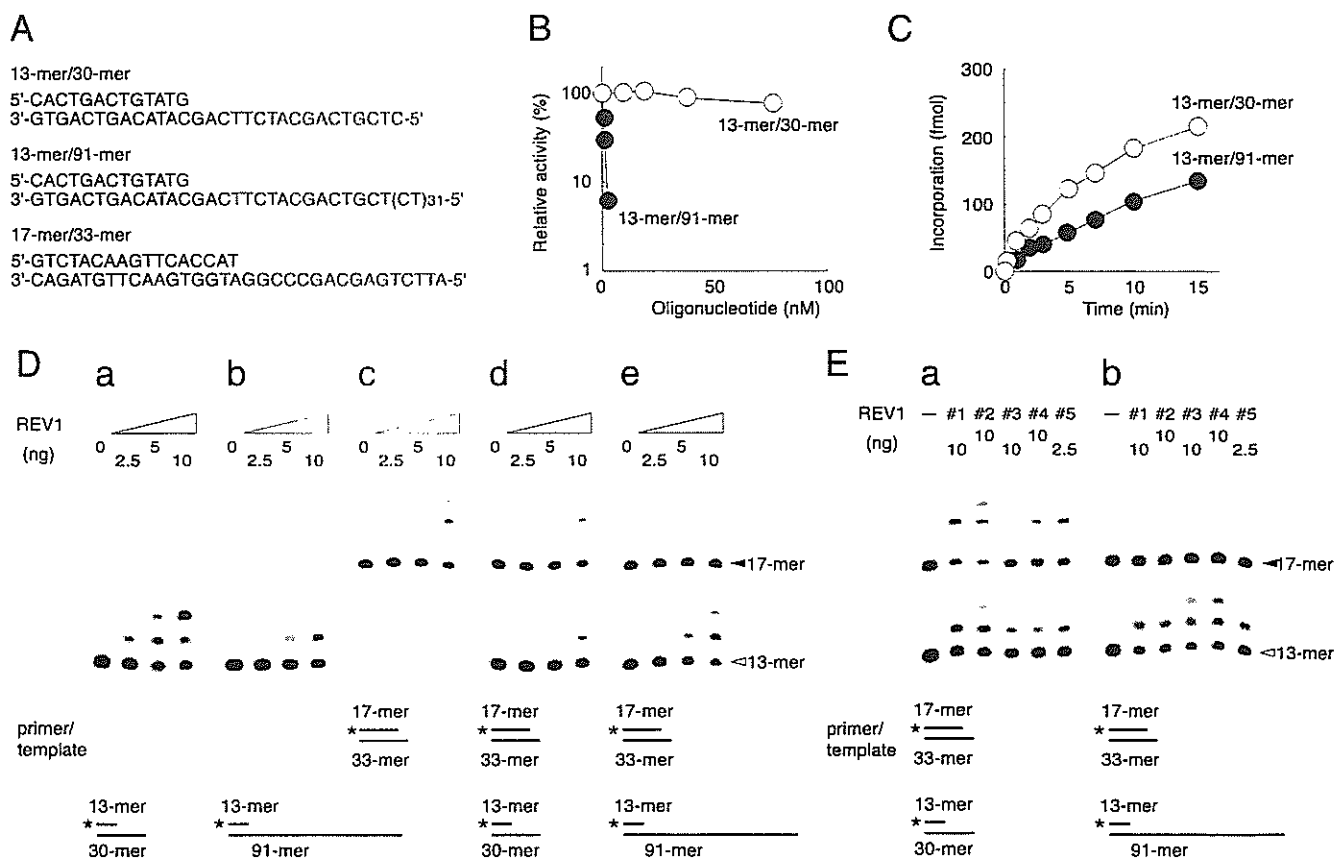


FIGURE 3. Template specificity of dCMP transferase reactions of REV1. *A*, nucleotide sequences of the primer-templates. *B*, inhibition of dCMP transferase activity of the REV1 protein by a primer-template containing long ssDNA. Ten ng of REV1 (2.8 nM) and the primer-template, P5786T (100 nM) as a substrate, were incubated under standard reaction conditions in the presence of the indicated concentration of 13/30- or 13/91-mer (*A*). Incorporation into the P5786T was measured and plotted in the graph. *C*, time course of dCMP transferase reactions using 13/30- and 13/91-mer (*A*) as substrates. REV1 (0.7 nM) and each primer-template (20 nM) were incubated for the indicated times. Incorporation into each 13-mer primer was measured. The errors in this assay were less than 5%. In the assays of *B* and *C*, the reaction products were resolved on 20% polyacrylamide gels containing 8 M urea, and amounts of DNA present in each band were quantified. *D* and *E*, competition assay of dCMP transferase activity using various primer-templates. The primer-templates shown in *A* (20 nM each) were used as substrates for the transferase assays (shown at the bottom of each panel) and were incubated with the indicated amount of REV1 (*D*) or deletion derivatives (*E*). The positions of 13- and 17-mer primer on the gels are shown by open and closed arrowheads, respectively. In the reactions with mixtures of two primer-templates, the respective primers were distinguished by differing size (panels *d* and *e* of *D*, and panels *a* and *b* of *E*). The reaction products migrating between 13- and 17-mer were derived from the 13-mer primer and those migrating larger than 17-mer were derived from the 17-mer primer. The molar concentrations of REV1 in the reactions were 0.7 nM (2.5 ng), 1.4 nM (5 ng), and 2.8 nM (10 ng), and those of mutant REV1 were 3.1 nM Δ 1 (10 ng), 3.8 nM Δ 2 (10 ng), 3.9 nM Δ 3 (10 ng), 4.2 nM Δ 4 (10 ng), and 1.8 nM Δ 5 (2.5 ng).

binding reaction, a primer-template was therefore introduced as a competitor. The result clearly demonstrated that the Δ 5-ssDNA complex was sensitive to addition of primer-template. The amount of the complex was decreased to 30% by addition of primer-template at 25 nM, indicating that the primer-template could access the catalytic site of Δ 5 even after complex formation with ssDNA. In contrast, we could not detect any difference between full-length REV1 and Δ 2, even though Δ 2 exhibited decreased sensitivity to ssDNA (Fig. 1G) as compared with full-length REV1. We consider that the difference could be due to sensitivity of the assay systems to detect competition between primer-template and ssDNA, but the results from both experiments were essentially consistent. From the results, we conclude that ssDNA binding itself does not fill up the catalytic site of the transferase but rather prevents accession of primer-template, and this function is because of the presence of N- and C-terminal domains.

Specific Utilization of a Primer-Template Containing Long ssDNA—For further investigation of this novel property of the REV1 protein, we addressed whether the catalytic site of the

transferase reaction might be accessible to a primer terminus annealed with a template containing a long ssDNA region (*cis* effect of ssDNA). Because the apparent binding affinity of REV1 to ssDNA is much higher than to the primer terminus (6), if the template contained a long ssDNA region, it could be a target for REV1 binding and inhibit the transferase reaction. To test this possibility, we made two primer-templates: one a 30-mer template annealed with a 13-mer primer, and the other a 91-mer template in which a dCT repeat was attached to the 5' end of the 30-mer, and the same 13-mer was annealed (Fig. 3A). First, we examined whether the primer-template could inhibit REV1 in an ssDNA-dependent manner when it was introduced in the reaction *in trans* (Fig. 3B). The transferase activity of REV1 was monitored using a different primer-template, P5786T. The result demonstrated that the oligonucleotide, 13/91-mer, inhibited transferase activity when introduced *in trans* (Fig. 3B), the effect being much stronger than that of poly[d(C-T)] 60-mer (Fig. 1E). This agreed with the synergistic properties (Fig. 1E), considering that the single-stranded region of 13/91-mer is 78 bases. This inhibition was not because of the structure

of primer-template, because it was not detected with 13/30-mer (Fig. 3B). Therefore, we concluded that the long ssDNA region in template acted as a target of REV1 binding and inhibited the activity.

We then labeled the primer termini of 13/30- and 13/91-mer with ^{32}P and examined the extensions (the *cis* effect of ssDNA) (Fig. 3C). Interestingly, both primer-templates were utilized as good substrates. The time courses of the reactions revealed that the incorporation of dCMP increased to a greater extent than the amount equivalent to REV1 protein (18 fmol) in the reaction solution, indicating REV1 was turned over many times. Thus, the catalytic site of the REV1 protein was accessible in *cis*, meaning that even after binding to ssDNA, REV1 interacted with a primer terminus that is located on the long ssDNA template.

To further confirm this property of REV1, we designed an experiment in which two primer-templates, one contained a long ssDNA in the template and the other contained a shorter ssDNA in the template, were competed with each other in the same reaction for utilization as substrates for REV1. To distinguish the reaction products on a polyacrylamide gel, we made another oligonucleotide, 17/33-mer composed of a different sequence with a short template strand (Fig. 3A). Because the 17-mer primer is 4 bases longer than the 13-mer primer, the reaction products derived from 17-mer could not be overlapped by the products derived from the 13-mer when those were reacted together in a mixture. Those primer-templates were utilized to almost the same extent in the transferase reactions (Fig. 3D, panels a–c). When the 13/30- and 17/33-mer were reacted with REV1 in one tube, both were utilized to the same extent (Fig. 3D, panel d). However, when the 13/91- and 17/33-mer were reacted with REV1 in one tube, we observed no extension of the 17-mer (Fig. 3D, panel e), indicating that REV1 specifically utilized the primer-template followed by long ssDNA.

When the same experiment was carried out using truncated mutants (Fig. 3E), the specific activities of mutant proteins slightly differed possibly due to variation in stability under standard reaction conditions. In this assay, we compared the proteins with equivalent levels of activity, rather than amount of proteins themselves (Fig. 3E). When 13/30- and 17/33-mer were reacted with mutant REV1 proteins in one tube, both primers were extended (Fig. 3E, panel a). With the 13/91- and 17/33-mer and mutants, the specificity to 13/91-mer was abolished only with the mutant $\Delta 5$ (Fig. 3E, panel b). This result agreed with inhibition curves of the mutants with ssDNA (Fig. 1G) and the electrophoretic mobility shift assay (Fig. 2, C and D). Thus, REV1 is specifically targeted to the primer terminus, followed by the long ssDNA template, and the N- and C-terminal regions are required for the activity.

Effects of ssDNA on DNA Polymerase Activity of pol α , β , and η —Although REV1 is one member of the Y family of DNA polymerases (14), the N- and C-terminal regions are not conserved. To determine whether the novel activity is specific to REV1, we first tested the inhibitory effects of ssDNA on another Y family polymerase, human pol η (42), and distinct family members, human pol α (B family) and β (X family) (49, 50). Neither of the polymerases was inhibited by d(C-T) $_{30}$, 60-mer, in contrast to REV1 (Fig. 4A). We also tested the specificity for primer-template following long ssDNA using combinations of 13/30- and 17/33-mer and 13/91- and 17/33-mer oligonucleotides (Fig. 4B). In this assay, the

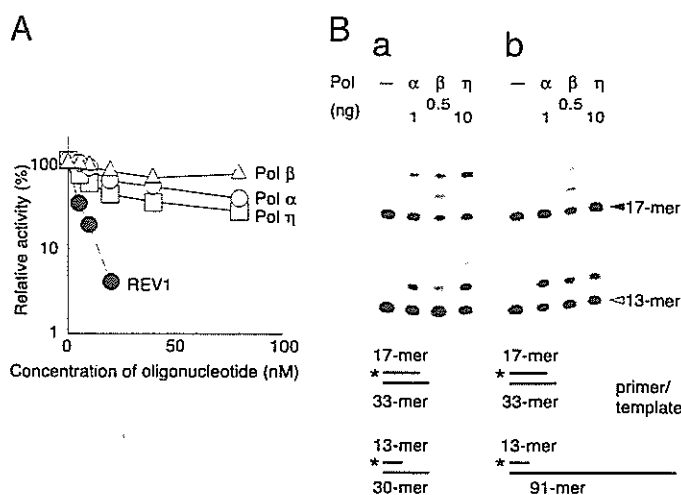


FIGURE 4. The targeting mechanism is REV1-specific. A, effects of ssDNA on DNA polymerase activity of pol α , β , and η . Relative activities were measured by incorporation of [α - ^{32}P]dCMP in a reaction mixture containing dNTP into unlabeled primer-template, P5786T, in the presence of various concentrations of d(C-T) $_{30}$ 60-mer. B, competition assay on the primer extension activity of DNA polymerases using various primer-templates. The primer-templates (20 nM each) shown in Fig. 3A were used as substrates for the primer extension assay. The indicated amounts of DNA polymerases and a mixture of a set of primer-template shown at the bottom of each panel were incubated with only dCTP, because further primer extensions of 13-mer by incorporation of dNTP would result in overlapping of products from 17-mer and make the results confusing. The reaction products were resolved on 20% polyacrylamide gels containing 8 M urea, and the amounts of DNA present in each band were quantified. The molar concentrations of polymerases in the reactions were 0.2 nM pol α (1 ng), 0.5 nM (0.5 ng of pol β) and 5 nM pol η (10 ng).

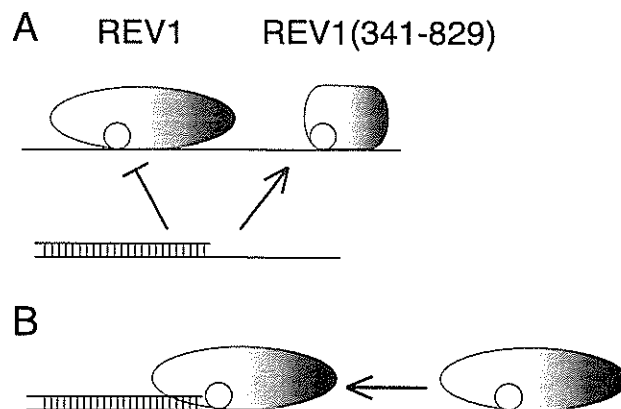


FIGURE 5. Model for actions of REV1. A, sequestration of REV1 from primer-template by ssDNA. B, targeting REV1 to a primer terminus via ssDNA binding. The catalytic site of REV1 is shown as an open circle inside shaded oval. See text for details.

primer extension reactions were carried out with only dCTP as the dNTP source to prevent overlapping reaction products. Although pol α and η showed a slight preference for 13/91-mer (Fig. 4B), the level was similar to that of $\Delta 5$ (Fig. 3E, panel b), suggesting that the novel property is REV1-specific.

DISCUSSION

In this study, we provide evidence of a novel biochemical activity of human REV1 protein. First, we found that ssDNA inhibits the transferase activity of REV1, because of sequestration of the catalytic site by high affinity binding (Fig. 5A). The N- and C-terminal domains are required for the sequestration, because a mutant REV1 lacking both N- and C-terminal

Targeting REV1 by Single-stranded DNA

domains lost only the function for sequestration, and not ssDNA binding and transferase activity (Fig. 5A). Second, we demonstrated that sequestration by ssDNA is only effective in *trans*. When REV1 binds to the template strand annealing a primer, the primer terminus is accessible for the catalytic site (Fig. 5B). Therefore, the catalytic site is open in *cis*. Third, we showed that REV1 preferentially utilizes the primer-template following long ssDNA.

We speculate that REV1 translocates on ssDNA from the following considerations, according to models involved in protein translocation that have been well discussed with regard to repressor-DNA recognition (51). We found that the extent of inhibition by ssDNA correlated with the length (Fig. 1E). To explain the synergism observed, two models were considered. One is a "dissociation-reassociation model," in which a protein dissociated from a DNA molecule could reassociate within a closely spaced site of the same DNA molecule. Therefore, the protein would appear to be trapped in the DNA molecule. The frequency of both initial binding and re-association would be proportional to the length of DNA. Because the binding event is affected by two factors, the inhibition curve would become "synergistic." The other is a "sliding model," in which the dissociation rate would be inversely proportional to the length of the DNA, because the protein could translocate at any point within the molecule. Besides, the length of the DNA molecule is proportional to the frequency of initial binding of the protein. Therefore, the inhibition curve would again become synergistic. After the occasional dissociation or sliding out of the DNA molecule, however, the protein could reassociate to another molecule of DNA, and therefore would not appear to be trapped. Our biochemical data here support the latter model. The primer-template following long ssDNA did not inhibit transferase activity in *cis*, and we observed turnover of REV1 protein several times with respect to dCMP transferase enzyme activity. These results indicate that after binding to any site of the ssDNA region, REV1 can access the primer terminus and subsequently dissociate and re-bind to another molecule. Currently, we do not have direct evidence for sliding of REV1, but we cannot explain our biochemical data without consideration of such translocation.

Translesion DNA synthesis plays an important role in post-replication repair pathways. It has been postulated that after posing a replicative DNA polymerase at a damage base, it is replaced with specialized DNA polymerases for translesion DNA synthesis. However, the biochemical reactions have yet to be clarified. Genetic data from yeast to humans suggest that REV1 has a central function in organizing such a polymerase switch (3). Besides, in higher eukaryotes, it has been shown that mouse and human REV1 have potential for interaction with other translesion DNA polymerases (35–41). The novel property of REV1 may play a role in organization of translesion DNA synthesis (52).

Acknowledgments—We thank Dr. Fumio Hanaoka (Osaka University, Osaka, Japan) and Dr. Motoshi Suzuki (Nagoya University, Nagoya, Japan) for providing the POLH cDNA and the POLA cDNA, respectively. We are grateful to Enko Aoki for help with cDNA cloning, and Kumiko Mizuno, Masako Oki, Miki Yano, and Hatsue Wakayama for their laboratory assistance.

REFERENCES

1. Lemontt, J. F. (1971) *Genetics* 68, 21–23
2. Lawrence, C. W., Das, G., and Christensen, R. B. (1985) *Mol. Gen. Genet.* 200, 80–85
3. Lawrence, C. W. (2002) *DNA Repair* 1, 425–435
4. Nelson, J. R., Lawrence, C. W., and Hinkle, D. C. (1996) *Nature* 382, 729–731
5. Nelson, J. R., Lawrence, C. W., and Hinkle, D. C. (1996) *Science* 272, 1646–1649
6. Masuda, Y., Takahashi, M., Tsunekuni, N., Minami, T., Sumii, M., Miyagawa, K., and Kamiya, K. (2001) *J. Biol. Chem.* 276, 15051–15058
7. Masuda, Y., Takahashi, M., Fukuda, S., Sumii, M., and Kamiya, K. (2002) *J. Biol. Chem.* 277, 3040–3046
8. Murakumo, Y., Roth, T., Ishii, H., Rasio, D., Numata, S., Croce, C. M., and Fishel, R. (2000) *J. Biol. Chem.* 275, 4391–4397
9. Gibbs, P. E., McGregor, W. G., Maher, V. M., Nisson, P., and Lawrence, C. W. (1998) *Proc. Natl. Acad. Sci. U. S. A.* 95, 6876–6880
10. Gibbs, P. E., Wang, X. D., Li, Z., McManus, T. P., McGregor, W. G., Lawrence, C. W., and Maher, V. M. (2000) *Proc. Natl. Acad. Sci. U. S. A.* 97, 4186–4191
11. Lin, W., Xin, H., Zhang, Y., Wu, X., Yuan, F., and Wang, Z. (1999) *Nucleic Acids Res.* 27, 4468–4475
12. Lin, W., Wu, X., and Wang, Z. (1999) *Mutat. Res.* 433, 89–98
13. Van Sloun, P. P., Romeijn, R. J., and Eeken, J. C. (1999) *Mutat. Res.* 433, 109–116
14. Ohmori, H., Friedberg, E. C., Fuchs, R. P., Goodman, M. F., Hanaoka, F., Hinkle, D., Kunkel, T. A., Lawrence, C. W., Livneh, Z., Nohmi, T., Prakash, L., Prakash, S., Todo, T., Walker, G. C., Wang, Z., and Woodgate, R. (2001) *Mol. Cell* 8, 7–8
15. Burgers, P. M., Koonin, E. V., Bruford, E., Blanco, L., Burtis, K. C., Christman, M. F., Copeland, W. C., Friedberg, E. C., Hanaoka, F., Hinkle, D. C., Lawrence, C. W., Nakanishi, M., Ohmori, H., Prakash, L., Prakash, S., Reynaud, C. A., Sugino, A., Todo, T., Wang, Z., Weill, J. C., and Woodgate, R. (2001) *J. Biol. Chem.* 276, 43487–43490
16. Haracska, L., Prakash, S., and Prakash, L. (2002) *J. Biol. Chem.* 277, 15546–15551
17. Masuda, Y., and Kamiya, K. (2002) *FEBS Lett.* 520, 88–92
18. Zhang, Y., Wu, X., Rechkoblit, O., Geacintov, N. E., Taylor, J. S., and Wang, Z. (2002) *Nucleic Acids Res.* 30, 1630–1638
19. Nair, D. T., Johnson, R. E., Prakash, L., Prakash, S., and Aggarwal, A. K. (2005) *Science* 309, 2219–2222
20. Gibbs, P. E., and Lawrence, C. W. (1995) *J. Mol. Biol.* 251, 229–236
21. Otsuka, C., Sanadai, S., Hata, Y., Okuto, H., Noskov, V. N., Loakes, D., and Negishi, K. (2002) *Nucleic Acids Res.* 30, 5129–5135
22. Zhao, B., Xie, Z., Shen, H., and Wang, Z. (2004) *Nucleic Acids Res.* 32, 3984–3994
23. Auerbach, P., Bennett, R. A., Bailey, E. A., Krokan, H. E., and Demple, B. (2005) *Proc. Natl. Acad. Sci. U. S. A.* 102, 17711–17716
24. Nelson, J. R., Gibbs, P. E., Nowicka, A. M., Hinkle, D. C., and Lawrence, C. W. (2000) *Mol. Microbiol.* 37, 549–554
25. Haracska, L., Unk, I., Johnson, R. E., Johansson, E., Burgers, P. M., Prakash, S., and Prakash, L. (2001) *Genes Dev.* 15, 945–954
26. Otsuka, C., Kobayashi, K., Kawaguchi, N., Kunitomi, N., Moriyama, K., Hata, Y., Iwai, S., Loakes, D., Noskov, V. N., Pavlov, Y., and Negishi, K. (2002) *Mutat. Res.* 502, 53–60
27. Otsuka, C., Kunitomi, N., Iwai, S., Loakes, D., and Negishi, K. (2005) *Mutat. Res.* 578, 79–87
28. Clark, D. R., Zacharias, W., Panaitescu, L., and McGregor, W. G. (2003) *Nucleic Acids Res.* 31, 4981–4988
29. Poltoratsky, V., Horton, J. K., Prasad, R., and Wilson, S. H. (2005) *DNA Repair* 4, 1182–1188
30. Jansen, J. G., and de Wind, N. (2003) *DNA Repair* 2, 1075–1085
31. Jansen, J. G., Tsaalbi-Shtylik, A., Langerak, P., Calleja, F., Meijers, C. M., Jacobs, H., and de Wind, N. (2005) *Nucleic Acids Res.* 33, 356–365
32. Simpson, L. J., and Sale, J. E. (2003) *EMBO J.* 22, 1654–1664
33. Okada, T., Sonoda, E., Yoshimura, M., Kawano, Y., Saya, H., Kohzaki, M., and Takeda, S. (2005) *Mol. Cell. Biol.* 25, 6103–6111

34. Ross, A. L., Simpson, L. J., and Sale, J. E. (2005) *Nucleic Acids Res.* **33**, 1280–1289
35. Murakumo, Y., Ogura, Y., Ishii, H., Numata, S., Ichihara, M., Croce, C. M., Fishel, R., and Takahashi, M. (2001) *J. Biol. Chem.* **276**, 35644–35651
36. Guo, C., Fischhaber, P. L., Luk-Paszyc, M. J., Masuda, Y., Zhou, J., Kamiya, K., Kisker, C., and Friedberg, E. C. (2003) *EMBO J.* **22**, 6621–6630
37. Ohashi, E., Murakumo, Y., Kanjo, N., Akagi, J., Masutani, C., Hanaoka, F., and Ohmori, H. (2004) *Genes Cells* **9**, 523–531
38. Tissier, A., Kannouche, P., Reck, M. P., Lehmann, A. R., Fuchs, R. P., and Cordonnier, A. (2004) *DNA Repair* **3**, 1503–1514
39. Masuda, Y., Ohmae, M., Masuda, K., and Kamiya, K. (2003) *J. Biol. Chem.* **278**, 12356–12360
40. Acharya, N., Haracska, L., Johnson, R. E., Unk, L., Prakash, S., and Prakash, L. (2005) *Mol. Cell. Biol.* **25**, 9734–9740
41. Guo, D., Xie, Z., Shen, H., Zhao, B., and Wang, Z. (2004) *Nucleic Acids Res.* **32**, 1122–1130
42. Masutani, C., Kusumoto, R., Yamada, A., Dohmae, N., Yokoi, M., Yuasa, M., Araki, M., Iwai, S., Takio, K., and Hanaoka, F. (1999) *Nature* **399**, 700–704
43. Niimi, A., Limsirichaikul, S., Yoshida, S., Iwai, S., Masutani, C., Hanaoka, F., Kool, E. T., Nishiyama, Y., and Suzuki, M. (2004) *Mol. Cell. Biol.* **24**, 2734–2746
44. Yasuda, S., and Takagi, T. (1983) *J. Bacteriol.* **154**, 1153–1161
45. Studier, F. W., Rosenberg, A. H., Dunn, J. J., and Dubendorff, J. W. (1990) *Methods Enzymol.* **185**, 60–89
46. Masuda, Y., Bennett, R. A., and Demple, B. (1998) *J. Biol. Chem.* **273**, 30352–30359
47. Gomes, X. V., Gary, S. L., and Burgers, P. M. (2000) *J. Biol. Chem.* **275**, 14541–14549
48. Sambrook, J., Fritsch, E. F., and Maniatis, T. (1989) *Molecular Cloning: A Laboratory Manual*, 2nd Ed., Cold Spring Harbor Laboratory Press, Appendix E.19, Cold Spring Harbor, NY
49. Braithwaite, D. K., and Ito, J. (1993) *Nucleic Acids Res.* **21**, 787–802
50. Aravind, L., and Koonin, E. V. (1999) *Nucleic Acids Res.* **27**, 1609–1618
51. Berg, O. G., Winter, R. B., and von Hippel, P. H. (1981) *Biochemistry* **20**, 6929–6948
52. Waters, L. S., and Walker, G. C. (2006) *Proc. Natl. Acad. Sci. U. S. A.* **103**, 8971–8976



ORIGINAL ARTICLE

HIV-1 Vpr induces ATM-dependent cellular signal with enhanced homologous recombination

C Nakai-Murakami¹, M Shimura¹, M Kinomoto², Y Takizawa³, K Tokunaga², T Taguchi¹, S Hoshino¹, K Miyagawa⁴, T Sata², H Kurumizaka³, A Yuo¹ and Y Ishizaka¹

¹Departments of Intractable Diseases and Hematology, International Medical Center of Japan, Shinjuku-ku, Tokyo, Japan;

²Department of Pathology, National Institute of Infectious Diseases, Shinjuku-ku, Tokyo, Japan; ³Waseda University School of Science and Engineering, Shinjuku-ku, Tokyo, Japan and ⁴Section of Radiation Biology, Graduate School of Medicine, The University of Tokyo, Bunkyo-ku, Tokyo, Japan

An ATM-dependent cellular signal, a DNA-damage response, has been shown to be involved during infection of human immunodeficiency virus type-1 (HIV-1), and a high incidence of malignant tumor development has been observed in HIV-1-positive patients. Vpr, an accessory gene product of HIV-1, delays the progression of the cell cycle at the G2/M phase, and ATR–Chk1–Wee-1, another DNA-damage signal, is a proposed cellular pathway responsible for the Vpr-induced cell cycle arrest. In this study, we present evidence that Vpr also activates ATM, and induces expression of γ -H2AX and phosphorylation of Chk2. Strikingly, Vpr was found to stimulate the focus formation of Rad51 and BRCA1, which are involved in repair of DNA double-strand breaks (DSBs) by homologous recombination (HR), and biochemical analysis revealed that Vpr dissociates the interaction of p53 and Rad51 in the chromatin fraction, as observed under irradiation-induced DSBs. Vpr was consistently found to increase the rate of HR in the locus of *I-SceI*, a rare cutting-enzyme site that had been introduced into the genome. An increase of the HR rate enhanced by Vpr was attenuated by an ATM inhibitor, KU55933, suggesting that Vpr-induced DSBs activate ATM-dependent cellular signal that enhances the intracellular recombination potential. In context with a recent report that KU55933 attenuated the integration of HIV-1 into host genomes, we discuss the possible role of Vpr-induced DSBs in viral integration and also in HIV-1 associated malignancy. *Oncogene* (2007) 26, 477–486. doi:10.1038/sj.onc.1209831; published online 18 September 2006

Keywords: HIV-1; Vpr; DNA double-strand breaks; homologous recombination; Non-AIDS defining malignancies

Correspondence: Dr Y Ishizaka, Department of Intractable Diseases, International Medical Center of Japan, 1-21-1 Toyama, Shinjuku-ku, Tokyo 162-8655, Japan.
E-mail: zakay@ri.imcj.go.jp
Received 22 August 2005; revised 12 May 2006; accepted 12 June 2006; published online 18 September 2006

Introduction

The induction of a cellular response similar to DNA-damage-sensing signals has been shown during human immunodeficiency virus type-1 (HIV-1) infection (Daniel *et al.*, 1999, 2003, 2004, 2005; Lau *et al.*, 2004). The synthesis of linear HIV-1 DNA in the cytoplasm by reverse transcription and the integration process of HIV-1 DNA into the host genome are thought to be possible triggers for the DNA-damage signals (Lau *et al.*, 2004, 2005). When chromosomal DNA is damaged (DSB; DNA double-strand break), two kinds of kinases (ATM and ATR) are initially activated to exert checkpoint control on cell cycle (Abraham, 2001). When caffeine, which is known to inhibit both ATR and ATM, is administered in conjugation with the viral infection, the integration of viral DNA into the host genome is impaired (Daniel *et al.*, 2005). Additionally, data showing that the recently developed ATM inhibitor KU55933 decreased the copy number of the integrated HIV-1 DNAs strongly suggest that an ATM-dependent signal has a key role in viral transduction (Lau *et al.*, 2005). In addition to the mechanism of viral infection, HIV-1-induced DSBs or their signals have an impact on the approaching AIDS pathogenesis, especially for cancer development. A high incidence of malignant tumors has been reported in AIDS patients (Mayer *et al.*, 1995; Biggar *et al.*, 1996; Straus, 2001), and recent observations have indicated that tumor development is observed even in HIV-1-positive patients who do not show any immunocompromised manifestations (Knowles, 2003). These data suggest that HIV-1 infection is by itself oncogenic (Laurence and Astrin, 1991), but the viral protein responsible for ATM activation during HIV-1 infection has not been well characterized.

Vpr, an accessory gene product of HIV-1, impairs the progression of the cell cycle at G2/M phase (He *et al.*, 1995; Goh *et al.*, 1998). Vpr is thought to inactivate Cdc2, which is a component of maturation-promoting factor, by phosphorylating tyrosine 15 (Bukrinsky and Adzhubei, 1999; Elder *et al.*, 2002). Recent studies have shown that Vpr-induced G2 arrest is attenuated by the introduction of *wee-1* siRNA or deletion of the *wee-1*

gene (Yuan *et al.*, 2004). Together with data on a dominant-negative mutant of ATR and its siRNA, ATR-Chk2-Wee-1 as a summarized signal pathway was postulated to be responsible for the Vpr-induced G2 arrest (Roshal *et al.*, 2003; Yuan *et al.*, 2004; Zimmerman *et al.*, 2004). As an earlier study demonstrated that ATM was not important for Vpr-induced G2 arrest (Bartz *et al.*, 1996), there have been no reports that describe the activation of ATM under Vpr expression. To investigate the Vpr-induced cell cycle abnormalities, we established a MIT-23 cell line, in which Vpr expression is tightly regulated by a tetracycline promoter (Shimura *et al.*, 1999b). We found that the continuous expression of Vpr induced the formation of TUNEL-positive micronuclei and increased the rate of gene amplification (Shimura *et al.*, 1999a), implying that Vpr induces DSBs. Through an analysis with a pulse-field gel electrophoresis on HIV-1 infected cells, we recently detected an altered migration pattern of high-molecular-weight genomic DNA (Tachiwana *et al.*, 2006), also implying that Vpr induces DSBs. Thus, it is now important to clarify whether a cellular response dependent on ATM, a kinase activated selectively by DSBs (O'Connell *et al.*, 2000; Khanna *et al.*, 2001; Shiloh, 2001), is really induced by Vpr, and if so, we need to determine whether Vpr is the major viral protein responsible for ATM activation.

DNA damage is induced by reactive oxygen species, ionizing radiation, and chemicals (Abraham, 2001), and are repaired by homologous recombination (HR) or nonhomologous DNA end-joining (NHEJ) pathways (Khanna and Jackson, 2001; van Gent *et al.*, 2001). Once a DSB is generated, a 3' single-stranded DNA tail is processed, where replication protein A (RPA) and Rad51, an eukaryotic homologue of the bacterial DNA strand exchange protein RecA (Cromie *et al.*, 2001; West, 2003), accumulate. It was shown that p53 and BRCA2 phosphorylated at serine 3291 bind Rad51 and suppress its HR activity (Dong *et al.*, 2003; Linke *et al.*, 2003; Yoon *et al.*, 2004). Functional BRCA1 and 2 are required when DSBs occur; otherwise, genomic instability is induced, as observed in cancer-prone individuals with mutations of these genes (van Gent *et al.*, 2001; Dong *et al.*, 2003).

In this report, we first show that Vpr induced an ATM-dependent cellular signal. The cellular response under Vpr expression was similar to that caused by X-ray irradiation involving BRCA1, RPA and Rad51. We next demonstrate that Vpr increased the frequency of HR in an ATM-dependent manner. Data support the idea that Vpr induces DSBs. The possible role of Vpr in viral infection and in HIV-1-associated malignant tumor development is discussed.

Results

DSB-induced cellular signals by Vpr

Initially, we examined whether DSB-dependent cellular signals were induced by HIV-1 infection. HT1080 cells

were infected with viruses without (R⁻) or with wild-type *vpr* (R⁺), and an immunohistochemical analysis was performed. As shown in Figure 1a, γ -H2AX accumulated after infection with the R⁺ virus (right panels) but not with the R⁻ virus (Figure 1a, middle panels). Western blot analysis demonstrated a high-level expression of γ -H2AX with the phosphorylation of p53 in cells infected with the R⁺ virus (Figure 1b, lanes 4 and 5). Viral concentrations of 50 and 100 ng/ml of p24 were sufficient for the induction of γ -H2AX. In contrast, the R⁻ virus did not induce p53 phosphorylation, although it slightly increased p53 expression (Figure 1b, lanes 2 and 3).

To characterize the intracellular signals specifically induced by Vpr, we used MIT-23 cells, in which *vpr* mRNA expression was tightly regulated by the tetracycline promoter (Shimura *et al.*, 1999b). In MIT-23 cells, Vpr expression was observed in 48 h after treatment of 3 μ g/ml of doxycycline (DOX) (Figure 2a). Under such conditions, we observed focus formation of ATM phosphorylated at serine 1981 (ATM-p) (Figure 2b, upper panels) and γ -H2AX (lower panels). In contrast, focus formation of these molecules was not observed in MIT-23 cells without DOX treatment (left panels). Additionally, we did not detect focus formation of

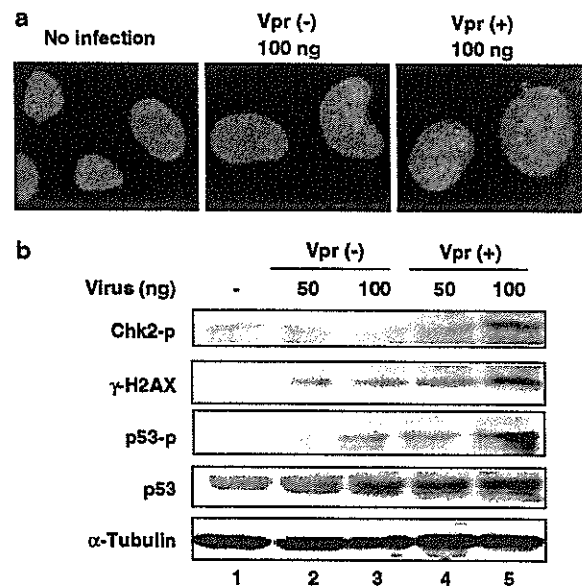


Figure 1 Activation of DSB-induced signaling. (a) Focus formation of γ -H2AX in cells infected with R⁻ or R⁺ virus. HT1080 cells were infected with R⁻ or R⁺ virus at the concentration of 100 ng/ml of p24 gag protein. After 48 h of infection, the cells were stained with specific antibody against γ -H2AX. The signals for γ -H2AX are shown as red spots in the nucleus (blue). (b) Western blot analysis of proteins involved in the DSB-induced signal pathway. Cell lysates of virus-infected and control cells after 48 h were subjected to analysis. Control cells (lane 1), cells infected with R⁻ virus (lanes 2 and 3), and cells infected with R⁺ virus (lanes 4 and 5) are shown. Two doses of viruses at the concentration of 50 (lanes 2 and 4) and 100 ng/ml of p24 gag protein (lanes 3 and 5) were used. α -Tubulin indicates that the amounts of loaded proteins are not significantly different.